

# Metal-phthalocyanine chains on the Au(110) surface: Interaction states versus *d*-metal states occupancy

Pierluigi Gargiani, Marco Angelucci, Carlo Mariani, and Maria Grazia Betti

*Dipartimento di Fisica, Università di Roma "La Sapienza," Piazzale A. Moro 5, I-00185 Roma, Italy*

(Received 9 October 2009; revised manuscript received 8 January 2010; published 8 February 2010)

The formation of long-range ordered organometallic structures has been demonstrated for metal-phthalocyanines (MPcs) with the metal *M* belonging to the 3*d* series (*M*=Fe,Co,Ni,Zn) deposited on the nanostructured template Au(110) by low-energy electron diffraction. The interaction of the molecular macrocycles of the regularly spaced MPc chains in the gold channels stabilizes the planar geometry, producing interface electronic states, as observed by high-resolution ultraviolet photoelectron spectroscopy. The MPc interaction with the substrate is further strengthened for FePc and CoPc molecules, where the central metal *d* orbitals are directly involved in the interaction process giving rise to interaction states close to the Fermi level.

DOI: [10.1103/PhysRevB.81.085412](https://doi.org/10.1103/PhysRevB.81.085412)

PACS number(s): 79.60.Dp, 73.20.-r

## I. INTRODUCTION

The huge interest in organic molecules as constituents of hybrid organic-inorganic interfaces is based on their flexibility and intriguing physical-chemical properties, when used as building blocks for the development of organic-based devices.<sup>1,2</sup> A general advance in the field of molecular manipulation is based on the engineering of suitable substrates for driving the organization of the molecular layers, allowing to produce artificially “frozen” configurations, robust enough to undergo reproducible experiments and possibly implementation of reliable functionalities. Metal-organic molecules can organize into periodic ordered arrays on well defined surfaces forming a variety of molecular one-dimensional (1D) and two-dimensional (2D) superstructures and allowing for tunable anchoring sites.<sup>3,4</sup> Metal-organic molecular architectures with well defined geometry and with high structural stability can constitute metal coordinated networks that may exhibit unusual magnetic phenomena depending on the central metal atom.<sup>5,6</sup> In fact, while individual atoms are difficult to immobilize regularly spaced on metal surfaces, the aromatic surrounding macrocycles can be suitable anchors to form ordered metal networks with high stability.

Highly ordered structures of flat-lying organic  $\pi$ -conjugated molecules have been obtained exploiting the step superstructure of metal vicinal surfaces<sup>7,8</sup> or exploiting metal reconstructed surfaces.<sup>9-12</sup> Metal-phthalocyanines [(MPcs) *M*-C<sub>32</sub>H<sub>16</sub>N<sub>8</sub>] are planar molecules formed by stable  $\pi$ -conjugated macrocycles coordinating a central metal atom. The mobility and charge delocalization are ensured by the  $\pi$  conjugation and the central metal atom can play a crucial role to establish the electronic/magnetic properties. Furthermore, the unique flexibility in coordinating more than 70 different metal atoms and the tendency to self-assemble on metal surfaces forming ordered aggregates make MPcs suitable to easily control the properties at the metal-organic/inorganic interface.<sup>13</sup> The adsorption of MPcs on metal and semiconductor surfaces produces long-range ordered single layers (SLs) with different interaction strengths depending on the competition between molecule-molecule and molecule-substrate interaction giving rise to different structural configurations at the interface. Numerous studies indi-

cate a planar MPc adsorption on different metal<sup>14-19</sup> and semiconductor<sup>20-23</sup> single-crystal surfaces suggesting a mixing of the molecular orbitals with the underlying substrate electronic states. Although the adsorption configurations are well known for several MPc molecules deposited on different substrates, the molecule-substrate interaction is still under debate especially regarding the nature of the interaction (chemisorption/physisorption) and the involvement of the central metal atoms. The role of the central metal atoms has been neglected, until spin-scattering processes were reported for MPc single-molecule adsorption on metallic surfaces,<sup>17,24,25</sup> opening the possibility to exploit the exchange interaction between the local magnetic moments of the spin center of the molecule and the underlying conducting electron gas. Further investigations on the metal center interaction with the substrates have been achieved by scanning tunneling microscopy (STM), where the observed variation in topography contrast in molecular centers between different MPcs has been attributed to the specific occupation of metallic *d*-orbital states.<sup>26,27</sup> Beyond the investigation of central magnetic/nonmagnetic atom in an isolated MPc molecule deposited on a surface, a detailed spectroscopic study of ordered MPc single layers, focusing on the role of the central metal atom in the molecule-substrate interaction, is still lacking.

In this paper, we report on a study of highly ordered metal-phthalocyanines with varying 3*d* metallic orbital occupancy assembled at a noble metal surface. Long-range ordering of the MPc structures is achieved by using pristine reconstructed Au(110)-(1×2) surface. The final goal is to control the interaction of these hybrid interfaces, in particular focusing on the role of the metal atom changing the 3*d* occupancy, from transition-metal atoms with a definite magnetic character to a filled *d* shell (*M*=Fe,Co,Ni,Zn).

## II. EXPERIMENTAL DETAILS

Experiments have been carried out at the surface physics laboratory LOTUS at the Università “La Sapienza,” Roma in an ultra-high-vacuum (UHV) chamber equipped with high-resolution ultraviolet photoelectron spectroscopy, low-energy electron diffraction (LEED), and all the ancillary facilities

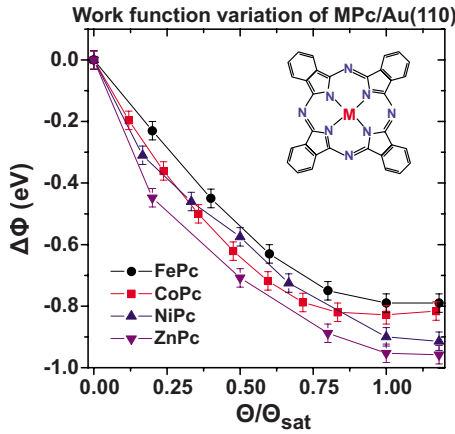


FIG. 1. (Color online) Work function variation as a function of MPC coverage on the Au(110) surface kept at 415 K. The saturation coverage  $\Theta_{\text{sat}}$  corresponds to establishment of the SL. The work function of the clean Au(110)-(1 $\times$ 2) is 5.31 eV. Inset: sketch of a MPC molecule.

for sample preparation. Photoelectron spectra have been excited with a He discharge lamp (He $I_{\alpha}$  and He $II_{\alpha}$  photons,  $h\nu=21.218$  eV and 40.814 eV, respectively). The photoemitted electrons were analyzed in the plane of incidence, with a high-resolution Scienta SES-200 hemispherical analyzer, by using a two-dimensional multi-channel-plate detector. Angular integration has been obtained over  $\pm 8^\circ$  around normal emission. The intrinsic energy resolution is 16 meV. A sharp long-range ordered (1 $\times$ 2) reconstruction pattern of the clean Au(110) surface was obtained by means of a double-step sputtering-annealing treatment (Ar $^+$  ions at 1000 eV,  $T=725$  K, followed by 500 eV–530 K). The MPC layers were prepared by evaporation from quartz crucibles after purification obtained by degassing cycles of several hours. The nominal thickness and the low deposition rate (less than 1 Å/min) were estimated by means of a quartz microbalance. The thickness of the first MPC layer is about 3.5 Å nominal coverage and it corresponds to completion of the first SL.

The MPC deposition has been calibrated controlling the work function variation ( $\Delta\Phi$ ) induced by MPC adsorption on the Au surface. The work function change has been determined by measuring the energy shift of the low-energy photoemission cutoff signal. A  $-9$  V bias has been applied to the sample with respect to ground, to measure the correct  $\Delta\Phi$ , avoiding any possible influence of the analyzer work function. The work function variation of the Au(110) surface upon MPC adsorption on the substrate kept at 415 K is shown in Fig. 1. For all MPCs, a decreasing drop in the work function at the initial stage of deposition is clearly displayed. In particular, the work function decreases by 0.79 eV (FePc), 0.83 eV (CoPc), 0.90 eV (NiPc), and 0.95 eV (ZnPc) at SL completion. The metal work function decreasing with the adsorption of  $\pi$ -conjugated molecules on metal surfaces has often been observed and it is generally attributed to the formation of an interface dipole<sup>28,29</sup> due to the highly polarizable metal electrons and caused by the  $\pi$  electrons approaching on the surface. The saturation in the work function

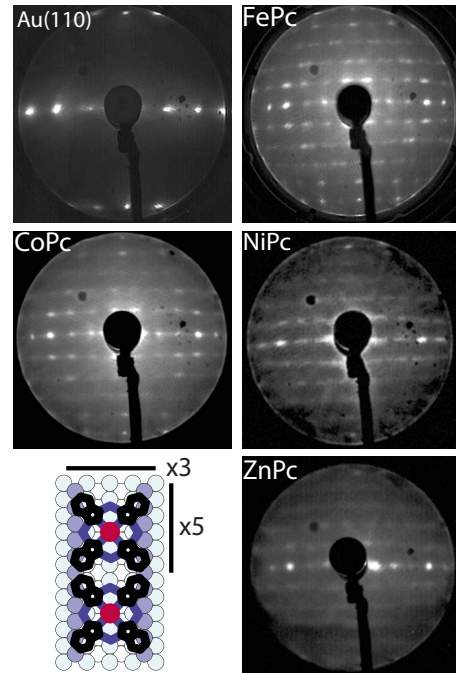


FIG. 2. (Color online) LEED patterns (primary beam energy 50 eV) of the (1 $\times$ 2)-Au(110) clean surface and of the (5 $\times$ 3) MPC ( $M=\text{Fe, Co, Ni, Zn}$ ) single layers. MPC molecules deposited on the Au(110) surface kept at 415 K. LEED data taken at 80 K. Bottom-left panel: sketch of the adsorption geometry of MPC on the Au(110) surface.

change, attained when the substrate is kept at about 415 K, corresponds to the formation of the ordered MPC SL.<sup>28</sup>

### III. RESULTS AND DISCUSSION

#### A. Metal-phthalocyanine chains on Au(110): Long-range ordering

Representative LEED patterns for the MPC ( $M=\text{Fe, Co, Ni, Zn}$ ) molecules deposited on the Au(110) surface kept at 415 K, at an incident electron energy of 50 eV, are shown in Fig. 2. The LEED patterns upon MPC deposition on the (1 $\times$ 2)-reconstructed Au(110) surface present sharp diffraction extra spots indicating a two-dimensional long-range ordering. Deposition on the substrate kept at room temperature (RT) gives rise to diffraction patterns with the same symmetry but with a diffuse background and a smearing of the spots.<sup>30</sup> The (1 $\times$ 2) symmetry of the Au(110) surface is due to the missing-row reconstruction (surface unit cell 2.884 Å $\times$ 8.156 Å). Upon MPC deposition onto the Au(110) surface kept at 415 K, the  $\times 2$  diffraction spots suddenly fade, while simultaneously pronounced 1/5 and 1/3 fractional order spots arise along the [1 $\bar{1}$ 0] and [001] symmetry directions, respectively, as shown in the spot profiles taken along the high-symmetry directions displayed in Fig. 3. The commensurate fivefold periodicity (14.40 Å) well fits the MPC size ( $\approx 13.8$  Å) considering the hypothesis of molecules flat lying on the underlying metal channels and lined up edge-to-edge along the [1 $\bar{1}$ 0] direction of the Au sub-

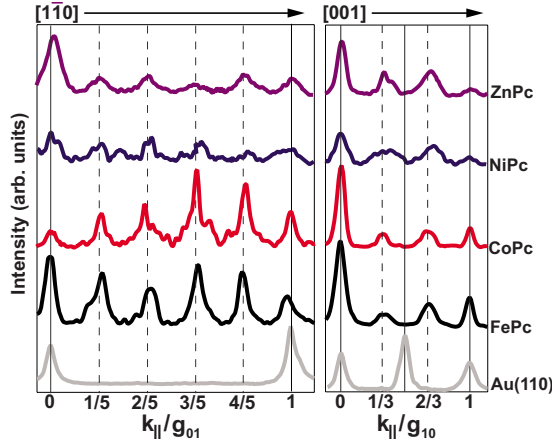


FIG. 3. (Color online) LEED spot profiles of MPc single layers grown on the Au(110) surface kept at 415 K taken along the  $[1\bar{1}0]$  and  $[001]$  symmetry directions.

strate. The SL attained with the  $(5 \times 3)$ -symmetry flat-lying molecules corresponds to a molecular density equivalent to  $1/15$  of the Au(110) atomic surface density ( $8.51 \times 10^{14}$  at./cm<sup>2</sup>). We can thus define one SL as constituted by about  $5.7 \times 10^{13}$  molecules/cm<sup>2</sup>. The formation of the Au reconstructed channels induced by the adsorption of  $\pi$ -conjugated planar organic molecules has been previously reported.<sup>9–12,31</sup> In particular, unidirectional  $\pi$ -stacked molecular chains aligned along the  $[1\bar{1}0]$  direction have been observed for the CuPc/Au(110) interface.<sup>11</sup> This configuration suggests that the threefold periodicity is mainly due to the Au substrate reconstruction, with an enlargement of the underlying Au channels, so as to easily accommodate the MPc chains. This geometrical configuration is favored by the low-energy difference among the Au(110)- $(1 \times n)$  reconstructions as predicted by total energy calculations.<sup>32</sup> This adsorption geometry (as sketched in the bottom-left panel of Fig. 2) with the  $(5 \times 3)$  symmetry is common to all these

MPc molecules deposited on the gold nanorails suggesting a secondary role exerted by the central metal atom in establishing the alignment of the MPc chains. Though, the nature of the interaction and the role of the central metal atoms can be better understood with an in-depth examination of the electronic state evolution upon changing the central metal atom in the MPc chains.

### B. Metal-phthalocyanine chains on Au(110): Electronic state evolution

In Fig. 4, we present normal-emission ultraviolet photoemission spectra in the valence-band energy region, for the MPc-Au(110) systems ( $M = \text{Fe}, \text{Co}, \text{Ni}, \text{Zn}$ ), as a function of molecular coverage. Data until formation of the first  $(5 \times 3)$  symmetry single layer are taken after deposition with the substrate kept at about 415 K. The SL coverage for all MPcs corresponds to the saturation of the work function and to the LEED patterns with a well defined  $(5 \times 3)$  reconstruction as shown in Fig. 2. Data at higher coverage are obtained with MPc deposition on the substrate kept at room temperature; in fact, the substrate at 415 K inhibits the growth of a thick molecular bulklike film as generally observed for  $\pi$ -conjugated molecular thin films governed by van der Waals molecular interactions.<sup>9</sup> The electronic states of the  $(5 \times 3)$  CuPc single layer deposited on Au(110) are reported in Ref. 33.

At first sight, the electronic spectral density is characterized by a similar evolution of the electronic features as a function of MPc coverage for all the present MPcs. In particular, at the first MPc deposition, the Au surface electronic states are quenched and electronic features of the hybrid interfaces appear in the energy region across the metal  $d$  bands up to the completion of the MPc long-range ordered single layers. The maximum intensity of the MPc-induced electronic states in the spectra occurs at formation of the single layers suggesting the localization of the MPc-induced states at the interfaces. All the MPc single layers present common

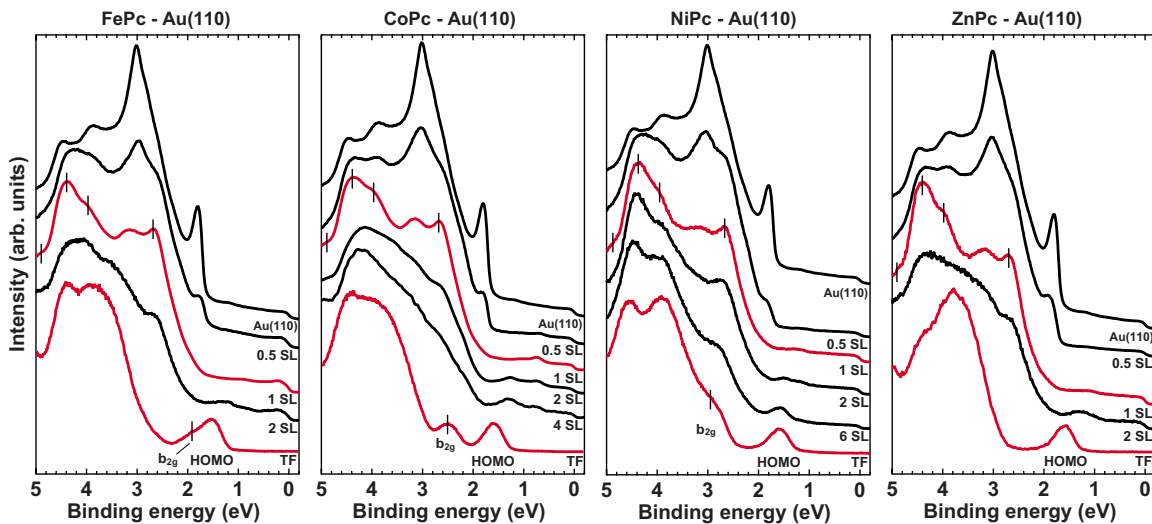


FIG. 4. (Color online) Normal-emission ultraviolet ( $h\nu = 21.218$  eV) photoemission spectra in the valence-band energy region as a function of MPc ( $M = \text{Fe}, \text{Co}, \text{Ni}, \text{Zn}$ ) coverage. One single layer corresponds to a molecular density of  $5.67 \times 10^{13}$  molecules/cm<sup>2</sup>. The thin film (TF) corresponds to about 30 nm thickness. Ticks mark the most relevant interface states.



$I_n$  interface states whose binding energy (BE) position is independent of the different central metal atoms at 2.70 eV ( $I_1$ ), 4.00 eV ( $I_2$ ), 4.40 eV ( $I_3$ ), and 4.92 eV ( $I_4$ ).

Further MPC deposition at RT induces an intensity decrease in the interface states, while the proper molecular levels of the MPC multilayers build up. The electronic spectral density reflects the energy distribution of the  $\pi$ ,  $\pi-\sigma$ , and  $\sigma$  molecular orbitals. In particular, the highest occupied molecular orbital (HOMO) with  $a_{1u}$  symmetry localized on the pyrrole ring is at a BE of 1.54 eV (FePc), 1.58 eV (CoPc), 1.58 eV (NiPc), and 1.57 eV (ZnPc) for the MPC thin films, once taken into account the different band bendings of the semiconducting MPC thin films. At higher binding energy, the molecular level  $b_{2g}$ , mainly localized on the central metal atoms,<sup>34</sup> is clearly identified at 1.91 eV (FePc), 2.43 eV (CoPc), and 2.97 eV (NiPc). Its assignment for CuPc (Ref. 33) and ZnPc is more ambiguous, because it shifts below the broad molecular structure centered at about 4 eV. The  $b_{2g}$  state presents an increasing binding energy, upon increasing the number of electrons in the 3d-metal central atom, while the  $a_{1u}$  molecular state, localized on the pyrrole ring, is almost unaffected by the metal substitution.

The comparison of the molecular electronic levels for the MPC thin films varying the central metal atoms is helpful to identify the origin of the interface states arising at the  $(5 \times 3)$  MPC single layers. Comparing the  $I_n$  electronic states with the proper molecular states in the 2–5 eV BE region, we do not observe a one-by-one correspondence. Thus, the interface states  $I_n$ , localized at the interface, can be attributed to macrocycle states resonating with Au bulk-projected bands,<sup>35</sup> whose density of states is redistributed due to interaction with the underlying Au surface,<sup>36</sup> which also causes the adsorption of the MPC SLs in a flat-lying configuration. In the case of the  $(5 \times 3)$  MPC-SLs on Au(110), the interaction cannot be simply interpreted as chemisorption or physisorption (pure van der Waals interaction), but there is a substrate-mediated interaction between these MPCs and Au, with a mixing of molecular and metal states producing surface dipole change and electronic state redistribution,<sup>33,36</sup> as in other  $\pi$ -conjugated oligomers interacting with the filled- $d$  band metal substrate.<sup>37–39</sup> The interaction between the molecule macrocycles with the underlying metallic states warrants the anchoring of the MPC molecules in the gold nano-rails, giving rise to an electronic spectral density common to all the MPC single layers, mainly due to a mixing of the  $\pi$ -molecular levels with the underlying metallic states. Furthermore, a fivefold electronic state dispersion of the  $I_1$  state along the molecular chains, as recently reported for the CuPc/Au(110)  $(5 \times 3)$ -reconstructed phase,<sup>33</sup> confirmed also for other MPC molecules (not shown here), corroborates this assumption.

A closer look in the low-BE region brings to light MPC-induced structures whose energy distribution clearly depends on the central metal atom. We present in Fig. 5 the high-resolution UV photoemission data for the  $(5 \times 3)$ -SL of each MPC. The more filled  $d$ -band MPCs ( $M=\text{Ni, Cu, Zn}$ ) present a tiny structure at about 1.2 eV for the single layer that fully develops in the HOMO with  $a_{1u}$  symmetry localized on the pyrrole ring for the TF. Thus, we can assign this peak to an interface-HOMO, as previously observed for the CuPc/

**(5x3)-MPC single-layer on Au(110)**

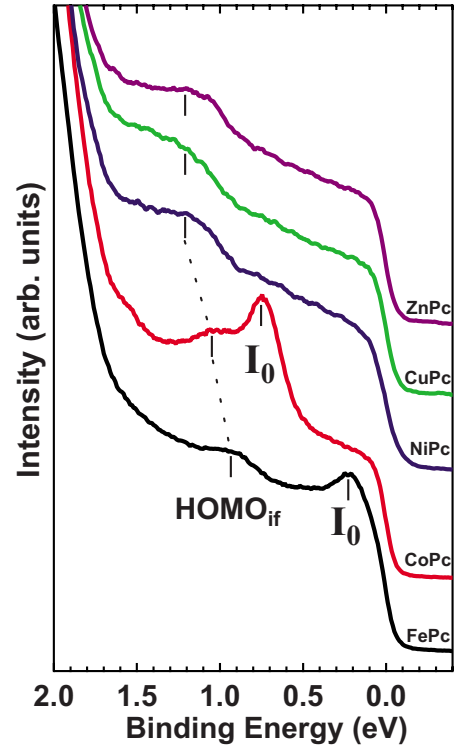


FIG. 5. (Color online) Normal-emission ultraviolet ( $h\nu = 21.218$  eV) photoemission spectra in the energy region close to the Fermi level for the MPC ( $M=\text{Fe, Co, Ni, Cu, Zn}$ ) single layers with  $(5 \times 3)$  symmetry.

Au(110) interface.<sup>33</sup> To better understand the more structured MPC-spectral density at the FePc and CoPc interfaces with Au, in Fig. 6 we report the coverage evolution of the electronic spectral density for FePc and CoPc, until formation of their respective TFs. The structures at 0.95 eV (FePc-SL) and 1.05 eV (CoPc-SL) are due to the interface-HOMO peaks localized on the pyrrole rings on the basis of their spectral evolution as a function of MPC thickness: their intensity is maximum at the SL completion, they fade at higher coverage, while the proper bulklike molecular HOMO fully develops. In the thin film, the  $a_{1u}$  state (HOMO) is clearly detectable, while the states localized on the central metal atom for the CoPc and FePc molecules are detectable only with an enhanced photoionization cross section for 3d orbitals,<sup>40</sup> as reported in previous photoemission experiments.<sup>41,42</sup> Data taken on the FePc and CoPc TFs with  $\text{He}_{II\alpha}$  radiation ( $h\nu = 40.814$  eV) are plotted as dotted lines on top of the corresponding  $\text{He}_{I\alpha}$  data (Fig. 6; bottom spectra). The  $\text{He}_{II\alpha}$  data are normalized to the intensity of the HOMO level of pure  $a_{1u}$  symmetry and an intensity increase of the shoulder at 1.91 eV present on the high-BE side of the HOMO is detectable for FePc. This evidence, along with the theoretically expected level ordering,<sup>34</sup> favors its assignment to the metal-associated  $b_{2g}$  state, which is present at 2.43 eV in the case of CoPc. A further lower intensity peak becomes observable at about 1.0 eV for CoPc upon increasing photon energy. It can be assigned to the single-occupied  $a_{1g}$  state in agreement with previous theoretical<sup>34</sup> and experimental<sup>42</sup> results.

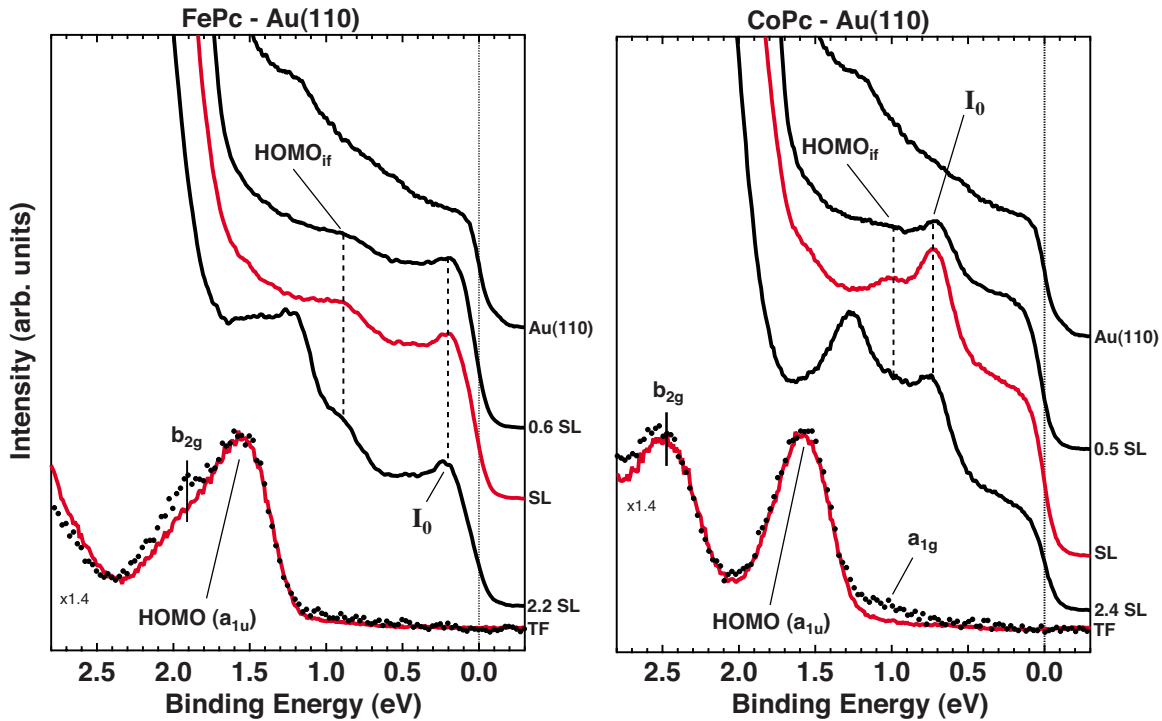


FIG. 6. (Color online) Normal-emission ultraviolet ( $\text{He}_{I\alpha}$ ,  $h\nu=21.218$  eV) photoemission spectra in the energy region close to the Fermi level for the FePc (left panel) and for CoPc (right panel) as a function of coverage. For both MPc thin films, superimposed to the data taken with  $\text{He}_{I\alpha}$  radiation, there are data excited with  $\text{He}_{II\alpha}$  photon energy  $h\nu=40.814$  eV (dotted lines) normalized to the  $\text{He}_{I\alpha}$  data.

We now discuss the  $I_0$  interface states at the FePc and CoPc SLs, also on the basis of the TF data. These states localized at 0.21 eV (FePc) and 0.73 eV (CoPc) are well defined and intense at the interfaces, then the intensity decreases and the peaks disappear after the formation of the thin semiconducting MPc films. Their attribution to a specific molecular-derived level is not straightforward, although they must be related with states residing on the central atoms, probably involved in the interaction with the underlying Au states. The evidence of interface states involving  $d$ -symmetry orbitals of the central metal Fe and Co atoms, close to the Fermi level, definitely explains the different apparent heights observed in the STM images of FePc and CoPc flat-lying molecules on Au(111), with respect to NiPc and CuPc.<sup>26,27</sup> The different  $d$ -orbital participation in these states close to the Fermi level does influence the apparent height measured in the filled density of states by STM. In fact, CoPc and FePc that have a consistent presence of  $d$ -symmetry states at low binding energy appear as molecular four-leaf patterns with a protruding center,<sup>26,27</sup> while NiPc and CuPc appear as four-leaf molecules with a slight central depression,<sup>26,27</sup> due to lack of  $d$  states in this energy region. FePc presents analogous but higher apparent STM image protrusion when adsorbed on Ag(111), where the interaction is stronger than with Au.<sup>43</sup> While these latter topographic investigations attributed the presence of these states localized on the metal to pure molecular levels, we assign the  $I_0$  interface state to  $d$  levels interacting with the underlying metal surface. In fact, the  $I_0$  intensity dependence as a function of the MPc thickness and the absence of a biunivocal correspondence between pure molecular and interface states in the

low-BE region favor the assumption of mixed MPc-Au states. This suggestion is in agreement with more recent data based on biased-dependent STM images of CoPc/Au(111),<sup>44,45</sup> where photoemission data from a CoPc-TF are compared to STM spectroscopy taken on a 2.8 Å-thick CoPc layer on the Au(111) surface.<sup>45</sup> It is more difficult to discriminate the specific molecular states localized on the central metal atoms responsible for this interaction process. Theoretical predictions<sup>34,46–52</sup> on the ground state of FePc and CoPc molecules are discordant on the energy distribution of the molecular levels mainly localized on the central metal atoms, with  $d$ -symmetry partially occupied orbitals. The transition-metal atoms, embedded in the molecular environment with a tetragonal symmetry, break the degenerate  $3d$  level symmetry giving rise to filled  $b_{2g}$  states with  $d_{xy}$  symmetry and the empty  $b_{1g}$  state with  $d_{x^2-y^2}$  symmetry, both hybridized with the  $\pi$  orbital localized on the nitrogen atoms, while the occupancy of the  $a_{1g}$  (mostly  $d_{z^2}$ ) and  $e_g$  (mostly  $d_{xy}, d_{xz}$ ) mainly localized on the magnetic atoms is still controversial, because it is strongly affected by the use of different exchange-correlation functionals, producing different energy positions and symmetry mixing.<sup>46,50–52</sup> However, these states are the candidates for explaining the presence of the interface states  $I_0$ . Thus, the  $I_0$  states localized at 0.21 eV and 0.73 eV, for the FePc/Au(110) and CoPc/Au(110) systems, respectively, can be due to a mixing of the  $a_{1g}/e_{1g}$  states hybridized with the  $\pi$  orbital localized on the N atoms, with the underlying Au metallic states. STM spectroscopy data<sup>45</sup> on 2.8 Å-CoPc/Au(111) also observe a tiny structure close to the Fermi level due to single-occupied  $a_{1g}$ -derived states, also observed in photoemission spectroscopy

copy for the CoPc TF, while inverse photoemission data identify as LUMO the  $a_{1g}$  close to the Fermi level for both FePc and CoPc.<sup>53</sup> Thus,  $I_0$  for the CoPc-SL can be assigned to the single-occupied  $a_{1g}$  state hybridized with the underlying Au states, while  $I_0$  for FePc-SL very close to the Fermi level can be due to charge transfer from the metal states to the formerly LUMO, whose symmetry is more difficult to univocally identify. In fact, we cannot exclude for  $I_0$  a contribution from  $e_g$  states very close in energy, while the empty  $b_{1g}$  lies far above the Fermi level.<sup>53</sup> The low symmetry environment of the MPc with central magnetic atoms on the Au(110) surface can break the symmetry of rehybridized  $a_{1g}$  and  $e_{1g}$  states, consequently inducing a reduced electronic magnetic moment, mainly due to the rehybridization of the single-occupied  $d_{z^2}$  state, as predicted by recent theoretical calculation for CoPc and FePc adsorption on the Au(111) surface.<sup>54</sup> In particular, a total quenching of the magnetic moment for CoPc adsorption has been computed and attributed to the interaction of the  $d_{z^2}$  states with Au for the CoPc/Au(111) interface.<sup>54</sup> All these considerations favor the hypothesis of state rehybridization upon FePc and CoPc interaction with Au involving molecular states with symmetry different from pure  $d$ -like. It is worth to note that, by using a higher photon energy (40.418 eV) enhancing the  $3d$  cross section, we do not observe an evident intensity increase in the  $I_0$  interface states for the FePc and CoPc SLs on the Au(110) surface, confirming their hybridized character with the underlying metal states.

The interaction of the FePc and CoPc chains with Au involves the metallic centers giving rise to molecular-induced states close to the Fermi level unlike the more  $d$ -filled MPc. Although the strength of the interaction appears

lower for NiPc, CuPc, and ZnPc, the geometry of the molecular adsorption seems basically unaffected, though only a detailed structural investigation can enlighten if the Fe and Co interaction influences the molecule-substrate distance.

#### IV. CONCLUSIONS

The capability to fabricate long-range ordered organometallic structures has been demonstrated for metal-phthalocyanines with the metal  $M$  belonging to the  $3d$  series ( $M=Fe, Co, Ni, Zn$ ) deposited on a suitable nanostructured template. The interaction between the molecule macrocycles with the Au(110) surface ensures the anchoring of the regularly spaced MPc in the gold channels giving rise to a spectral density in photoemission mainly due to a mixing of the molecular states with the underlying metallic states. This molecular geometry allows the formation of  $3d$  metallic centers with nanometer distances controlled by the molecular spacing with a  $(5 \times 3)$  symmetry. While Ni, Cu,<sup>33</sup> and Zn metallic centers do not directly interact with the underlying Au substrate, transition-metal center atoms such as Fe and Co induce interaction states close to the Fermi level. The interaction of the regularly spaced Fe and Co metallic centers with a nonmagnetic substrate (Au) can break the symmetry of the metallic  $d$  orbital carrying the magnetic moment giving rise to reduced magnetic moments. These states localized on the regularly spaced metal-organic chains can open a new scenario of further investigations exploiting the interrelationship between metal-metal spacing and metal-substrate interaction, with the final objective of controlling the electronic and magnetic properties of 2D metallic arrays or 1D chains.

<sup>1</sup>Z. Bao, A. J. Lovinger, and A. Dodabalapur, *Appl. Phys. Lett.* **69**, 3066 (1996).

<sup>2</sup>S. R. Forrest, *Nature (London)* **428**, 911 (2004).

<sup>3</sup>J. V. Barth, G. Costantini, and K. Kern, *Nature (London)* **437**, 671 (2005).

<sup>4</sup>F. Rosei, M. Schunack, Y. Naitoh, P. Jiang, A. Gourdon, E. Laegsgaard, I. Stensgaard, C. Joachim, and F. Besenbacher, *Prog. Surf. Sci.* **71**, 95 (2003).

<sup>5</sup>P. Gambardella, S. Stepanow, A. Dmitriev, J. Honolka, F. M. F. de Groot, M. Lingenfelder, S. S. Gupta, D. D. Sarma, P. Bencok, and S. Stanescu, *Nature Mater.* **8**, 189 (2009).

<sup>6</sup>H. Wende, M. Bernien, J. Luo, C. Sorg, N. Ponpandian, J. Kurde, J. Miguel, M. Piantek, X. Xu, and P. Eckhold, *Nature Mater.* **6**, 516 (2007).

<sup>7</sup>L. Gavioli, M. Fanetti, M. Sancrotti, and M. G. Betti, *Phys. Rev. B* **72**, 035458 (2005).

<sup>8</sup>J. Kröger, N. Néel, H. Jensen, R. Berndt, R. Rurai, and N. Lorente, *J. Phys.: Condens. Matter* **18**, S51 (2006).

<sup>9</sup>C. Baldacchini, C. Mariani, and M. G. Betti, *J. Chem. Phys.* **124**, 154702 (2006).

<sup>10</sup>F. Evangelista, A. Ruocco, D. Pasca, C. Baldacchini, M. G. Betti, V. Corradini, and C. Mariani, *Surf. Sci.* **566-568**, 79 (2004).

<sup>11</sup>L. Floreano, A. Cossaro, R. Gotter, A. Verdini, G. Bavdek, F. Evangelista, A. Ruocco, A. Morgante, and D. Cvetko, *J. Phys. Chem. C* **112**, 10794-10802 (2008).

<sup>12</sup>S. Prato, L. Floreano, D. Cvetko, V. D. Renzi, A. Morgante, S. Modesti, F. Biscarini, R. Zamboni, and C. Taliani, *J. Phys. Chem. B* **103**, 7788 (1999).

<sup>13</sup>H. Peisert, X. Liu, D. Olligs, A. Petr, L. Dunsch, T. Schmidt, T. Chassé, and M. Knupfer, *J. Appl. Phys.* **96**, 4009 (2004).

<sup>14</sup>S. H. Chang, S. Kuck, J. Brede, L. Lichtenstein, G. Hoffmann, and R. Wiesendanger, *Phys. Rev. B* **78**, 233409 (2008).

<sup>15</sup>P. Palmgren, T. Angot, C. I. Nlebedim, J. M. Layet, G. Le Lay, and M. Göthelid, *J. Chem. Phys.* **128**, 064702 (2008).

<sup>16</sup>P. Amsalem, L. Giovanelli, J. M. Themlin, and T. Angot, *Phys. Rev. B* **79**, 235426 (2009).

<sup>17</sup>A. Zhao, Q. Li, L. Chen, H. Xiang, W. Wang, S. Pan, B. Wang, X. Xiao, J. Yang, and J. G. Hou, *Science* **309**, 1542 (2005).

<sup>18</sup>A. Ruocco, F. Evangelista, A. Attili, M. P. Donzello, M. G. Betti, L. Giovanelli, and R. Gotter, *J. Electron Spectrosc. Relat. Phenom.* **137-140**, 165 (2004).

<sup>19</sup>A. Ruocco, F. Evangelista, R. Gotter, A. Attili, and G. Stefani, *J. Phys. Chem. C* **112**, 2016 (2008).

<sup>20</sup>N. Papageorgiou, Y. Ferro, J. M. Layet, L. Giovanelli, A. J. Mayne, G. Dujardin, H. Oughaddou, and G. Le Lay, *Appl. Phys.*

- Lett. **82**, 2518 (2003).
- <sup>21</sup>T. Angot, E. Salomon, N. Papageorgiou, and J. Layet, *Surf. Sci.* **572**, 59 (2004).
- <sup>22</sup>G. Dufour, C. Poncey, F. Rochet, H. Roulet, M. Sacchi, M. De-Santis, and M. Decrescenzi, *Surf. Sci.* **319**, 251 (1994).
- <sup>23</sup>E. Salomon, N. Papageorgiou, T. Angot, A. Verdini, A. Cossaro, L. Floreano, A. Morgante, L. Giovanelli, and G. Le Lay, *J. Phys. Chem. C* **111**, 12467 (2007).
- <sup>24</sup>Y.-S. Fu, S.-H. Ji, X. Chen, X.-C. Ma, R. Wu, C.-C. Wang, W.-H. Duan, X.-H. Qiu, B. Sun, P. Zhang, J. F. Jia, and Q. K. Xue, *Phys. Rev. Lett.* **99**, 256601 (2007).
- <sup>25</sup>L. Gao, W. Ji, Y. B. Hu, Z. H. Cheng, Z. T. Deng, Q. Liu, N. Jiang, X. Lin, W. Guo, S. X. Du, W. A. Hofer, X. C. Xie, and H. J. Gao, *Phys. Rev. Lett.* **99**, 106402 (2007).
- <sup>26</sup>X. Lu, K. W. Hipps, X. D. Wang, and U. Mazur, *J. Am. Chem. Soc.* **118**, 7197 (1996).
- <sup>27</sup>X. Lu and K. W. Hipps, *J. Phys. Chem. B* **101**, 5391 (1997).
- <sup>28</sup>T. S. Ellis, K. T. Park, S. L. Hulbert, M. D. Ulrich, and J. E. Rowe, *J. Appl. Phys.* **95**, 982 (2004).
- <sup>29</sup>W. Gao and A. Kahn, *J. Phys.: Condens. Matter* **15**, S2757 (2003).
- <sup>30</sup>F. Evangelista, A. Ruocco, V. Corradini, M. P. Donzello, C. Mariani, and M. G. Betti, *Surf. Sci.* **531**, 123 (2003).
- <sup>31</sup>V. Corradini, C. Menozzi, M. Cavallini, F. Biscarini, M. G. Betti, and C. Mariani, *Surf. Sci.* **532-535**, 249 (2003).
- <sup>32</sup>M. Garofalo, E. Tosatti, and F. Ercolessi, *Surf. Sci.* **188**, 321 (1987).
- <sup>33</sup>F. Evangelista, A. Ruocco, R. Gotter, A. Cossaro, L. Floreano, A. Morgante, F. Crispoldi, M. G. Betti, and C. Mariani, *J. Chem. Phys.* **131**, 174710 (2009).
- <sup>34</sup>M.-S. Liao and S. Scheiner, *J. Chem. Phys.* **114**, 9780 (2001).
- <sup>35</sup>T. Yokoya, A. Chainani, and T. Takahashi, *Phys. Rev. B* **55**, 5574 (1997).
- <sup>36</sup>H. Vázquez, W. Gao, F. Flores, and A. Kahn, *Phys. Rev. B* **71**, 041306(R) (2005).
- <sup>37</sup>A. Ferretti, C. Baldacchini, A. Calzolari, R. Di Felice, A. Ruini, E. Molinari, and M. G. Betti, *Phys. Rev. Lett.* **99**, 046802 (2007).
- <sup>38</sup>L. Huang, D. Rocca, S. Baroni, K. E. Gubbins, and M. B. Nardelli, *J. Chem. Phys.* **130**, 194701 (2009).
- <sup>39</sup>C. Baldacchini, C. Mariani, M. G. Betti, I. Vobornik, J. Fujii, E. Annese, G. Rossi, A. Ferretti, A. Calzolari, R. Di Felice, A. Ruini, and E. Molinari, *Phys. Rev. B* **76**, 245430 (2007).
- <sup>40</sup>J. J. Yeh and I. Lindau, *At. Data Nucl. Data Tables* **32**, 1 (1985).
- <sup>41</sup>T. S. Ellis, K. T. Park, M. D. Ulrich, S. L. Hulbert, and J. E. Rowe, *J. Appl. Phys.* **100**, 093515 (2006).
- <sup>42</sup>M. Grobosch, V. Yu. Aristov, O. V. Molodtsova, C. Schmidt, B. P. Doyle, S. Nannarone, and M. Knupfer, *J. Phys. Chem. C* **113**, 13219 (2009).
- <sup>43</sup>T. Takami, C. Carrizales, and K. V. Hipps, *Surf. Sci.* **603**, 3201 (2009).
- <sup>44</sup>M. Takada and H. Tada, *Chem. Phys. Lett.* **392**, 265 (2004).
- <sup>45</sup>Dan E. Barlow, L. Scudiero, and K. W. Hipps, *Langmuir* **20**, 4413 (2004).
- <sup>46</sup>A. Calzolari, A. Ferretti, and M. B. Nardelli, *Nanotechnology* **18**, 424013 (2007).
- <sup>47</sup>P. A. Reynolds and B. N. Figgis, *Inorg. Chem.* **30**, 2294 (1991).
- <sup>48</sup>T. Kroll, V. Yu. Aristov, O. V. Molodtsova, Y. Ossipyan, D. V. Vyalikh, B. Büchner, and M. Knupfer, *J. Phys. Chem. A* **113**, 8917 (2009).
- <sup>49</sup>A. Rosa and E. J. Baerends, *Inorg. Chem.* **33**, 584 (1994).
- <sup>50</sup>N. Marom and L. Kronik, *Appl. Phys. A: Mater. Sci. Process.* **95**, 165 (2009).
- <sup>51</sup>N. Marom and L. Kronik, *Appl. Phys. A: Mater. Sci. Process.* **95**, 159 (2009).
- <sup>52</sup>M. D. Kuz'min, R. Hayn, and V. Oison, *Phys. Rev. B* **79**, 024413 (2009).
- <sup>53</sup>N. Sato, H. Yoshida, and K. Tsutsumi, *Synth. Met.* **133-134**, 673 (2003).
- <sup>54</sup>Z. Hu, B. Li, A. Zhao, J. Yang, and J. G. Hou, *J. Phys. Chem. C* **112**, 13650 (2008).